PETROGRAPHIC EXAMINATION OF CONCRETE SAMPLES

GEO REPORT No. 119

R.J. Sewell & S.D.G. Campbell

GEOTECHNICAL ENGINEERING OFFICE
CIVIL ENGINEERING DEPARTMENT
THE GOVERNMENT OF THE HONG KONG SPECIAL ADMINISTRATIVE REGION

PETROGRAPHIC EXAMINATION OF CONCRETE SAMPLES

GEO REPORT No. 119

R.J. Sewell & S.D.G. Campbell

First published, October 2001

Prepared by:

Geotechnical Engineering Office,
Civil Engineering Department,
Civil Engineering Building,
101 Princess Margaret Road,
Homantin, Kowloon,
Hong Kong.

PREFACE

In keeping with our policy of releasing information which may be of general interest to the geotechnical profession and the public, we make available selected internal reports in a series of publications termed the GEO Report series. A charge is made to cover the cost of printing.

The Geotechnical Engineering Office also publishes guidance documents as GEO Publications. These publications and the GEO Reports may be obtained from the Government's Information Services Department. Information on how to purchase these documents is given on the last page of this report.

R.K.S. Chan
Head, Geotechnical Engineering Office
October 2001

EXPLANATORY NOTE

This GEO Report consists of three Geological Reports prepared by the Planning Division of the Geotechnical Engineering Office. The Geological Reports, which contain results of petrographic examination of thin sections of concrete from three different sites, are presented in three separate sections in this Report. Their titles are as follows:

SECTION 1: PETROGRAPHIC EXAMINATION OF CONCRETE CORES FROM FANLING FOOTBRIDGE

R.J. Sewell

This report was originally produced in October 2000 as GEO Geological Report No. GR 2/2000

FOREWORD

This report describes the results of a petrographic examination of sixteen thin sections of concrete suspected of having AAR. The samples were prepared from core samples taken from a footbridge near Fanling KCR Station. The study has been carried out in accordance with ASTM C856-95 to identify any potential AAR constituents and was written by Dr R.J. Sewell of the Geological Survey Section in the Planning Division.

(H.N. Wong)
Chief Geotechnical Engineer/Planning

CONTENTS

1. INTRODUCTION

Sixteen concrete thin sections and polished slabs were submitted to the Geological Survey Section of Planning Division for petrographic analysis in order to identify any potential Alkali-Aggregate Reaction (AAR) constituents. The thin sections and polished slabs were prepared from core samples taken from a footbridge near Fanling KCR Station which is suspected of having alkali-aggregate reaction. Since no details were given of the field characteristics of the concrete, the findings of this report are based solely on the petrographic observations.

Four concrete cores were used in the selection of samples. Two samples from each core were taken generally within 10-20 mm of the surface of the concrete, and two samples were taken at a depth of 90-120 mm from the surface.

2. PETROGRAPHIC EXAMINATION OF HARDENED CONCRETE

Petrographic examination of concrete is now commonly used for identification of alkali-aggregate reaction products and the standard procedures for such examination are outlined in ASTM C856-95 (ASTM, 1996a). Alkali-aggregate reaction occurs when minerals in certain aggregates react with the soluble alkaline components of the cement paste. Two main forms of alkali-aggregate reaction have been recognised: alkali-silica reaction and alkali-carbonate reaction. Except where dolomitic limestone has been used as an aggregate, most alkali-aggregate reaction is between alkaline components in the cement paste and reactive silica-bearing minerals in the accompanying aggregate.

3. IDENTIFICATION OF ALKALI-AGGREGATE REACTION IN THIN SECTION AND POLISHED SLABS

The general procedures adopted in this report for identification of alkali-aggregate reaction involved visual examination of polished slabs under a binocular microscope, followed by detailed examination of thin sections under a polarizing microscope. The macroscopic examination of the concrete included inspection for any obvious deleterious effects such as cracking, bleeding, void infilling, and carbonation. In addition, the size range, shape and type of aggregate fragments were described, along with any unusual features in the aggregate, such as the presence or absence of foliation, strained quartz, recrystallization and/or mineralization. Thin section examination was undertaken to identify the different varieties of aggregate fragments, and to determine any microscopic evidence for alkali-aggregate reaction. Features used to confirm the presence of alkali-aggregate reaction included the presence of gel filling cracks through the cement paste, gel filling cracks across grain boundaries and gel filling cracks on the margins of aggregate fragments.

4. LABORATORY INVESTIGATION

4.1 Description of Samples

Details of the depths of each of the examined samples measured from the wall surface of the concrete core are given in Table 1, while detailed petrographic descriptions are given in

Appendix 1. For ease of reference, the four core samples are referred to here as C, D, E and G. Except for core D, the distribution, size, shape, and composition of the aggregate populations in each of the cores are similar. Two fractions of aggregate fragments are generally present: coarse and fine. The coarse aggregate consists of 10-20 mm fragments of mainly coarse ash crystal metatuff, whereas the fine aggregate consists of 5-8 mm fragments of medium- and coarse-grained granite. Sporadic rhyolite and tuff fragments are also present. In core D, both coarse and fine aggregate fractions are composed of coarse ash crystal tuff. The interstitial sand size fraction is composed mostly of monocrystalline or polycrystalline quartz. There is no obvious possolanic additive in the concrete. The aggregate/binder ratio generally lies between 20/80 and 30/70, whereas flakiness is low to moderate in both size fractions. Pyrite is visible in the coarse aggregate fragments of many samples.

4.2 Petrographic Examination

The coarse aggregate fraction in all examined samples consists of coarse ash crystal metatuff with a moderate to strong metamorphic fabric. Metamorphism has resulted in recrystallization of matrix minerals, growth of oriented biotite, carbonate replacement, sericitization of feldspars and straining of quartz phenocrysts. Iron mineralization, which may have accompanied metamorphism, is present in the form of pyrite which has well-developed cubic crystal form. The fine aggregate fraction consists mostly of medium- and coarse-grained granite. Some granite fragments show evidence of recrystallization with growth of secondary muscovite although, in general, they are unmetamorphosed. Rare basalt and porphyritic rhyolite lava fragments are present in the fine aggregate fraction. The sand fraction consists of quartz grains, probably derived from a granitic source.

4.2.1 Core C

Samples within 10-20 mm from the concrete surface show evidence of reaction with atmospheric carbon dioxide as indicated by patches of strongly carbonated cement paste. Less carbonation is shown at deeper levels in the concrete. There is no obvious alkali-aggregate reaction in any of the Core C samples although thin microcracks were observed leading from coarse aggregate particles in Sample A2A (Plate 1). The concrete has moderate porosity as shown by penetration of resin into voids and matrix.

4.2.2 Core D

The coarse and fine aggregate particles in Core D are composed of coarse ash crystal metatuff. Samples within 10-20 mm of the surface are deeply carbonated with microcracks commonly surrounded by carbonated cement paste. These microcracks connect with voids and are probably associated with shrinkage. At deeper levels in the concrete (94-114 mm), microcracks are partly infilled with gel and surrounded by carbonated cement (Plate 2). The source of the silica gel is not clear but the common occurrence of veins on the surface of coarse aggregate fragments suggests the silica gel may have been derived from reacting aggregate.

4.2.3 Core E

The coarse aggregate particles in Core E are composed of coarse ash crystal metatuff, whereas the fine aggregate particles are composed principally of medium- and coarse-grained granite. Minor pyrite is present in many of the tuff fragments. Samples close to the surface (10-20 mm) are strongly carbonated. Microcracks are common, cutting through the cement paste and aggregate fragments, and form gaps around the margins of aggregate fragments (Plate 3). Microcracks also penetrate to deeper levels of the concrete (95-115 mm from surface) providing a conduit for reaction with atmospheric carbon dioxide as displayed by zones of carbonation surrounding these cracks. At these deeper levels, the microcracks are also partly infilled with silica gel (Plate 4).

4.2.4 Core G

The coarse aggregate fragments of Core G are composed of coarse ash crystal metatuff, whereas the fine aggregate particles consist of medium- and coarse-grained granite, minor basalt, and rhyolite fragments. At shallow levels (10-20 mm from surface) the cement paste is strongly carbonated. Microcracks are abundant along aggregate grain boundaries, interlinking with voids in the cement paste, and commonly surrounded by carbonated paste (Plates 5a and 5b). Some cracks are also partly infilled with silica gel. At deeper levels (70-90 mm from surface), microcracks are less common, but silica gel is more conspicuous, particularly along aggregate boundaries and infilling thin veins (Plate 6). These gel-infilled veins appear to originate from the coarse aggregate particles (metatuff fragments). Carbonation of the cement paste and minor ettringite formation are also associated with these veins.

4.3 Discussion of Results

The petrographic examination of the concrete cores from a footbridge near the Fanling KCR Station has established that coarse ash crystal metatuff is the principal coarse aggregate component, whereas medium and coarse grained granite is the main fine aggregate constitute. The metatuff is strongly altered and partly mineralized. Recrystallization of the matrix has generated abundant microcrystalline quartz, which together with strained quartz phenocrysts, provides potential ingredients for alkali-aggregate reaction (DOT, 1991; RILEM, 1993). Additional problematic components, such as the presence of carbonate and iron sulphide (pyrite) in the coarse aggregate fragments, also provide potential for defects in the concrete (see ASTM, 1996b). For example, iron sulphide may oxidise expansively and generate sulphates which react in the presence of water to produce ettringite (Midgely, 1958). At shallow levels (i.e. 10-20 mm from the surface), the cement paste has undergone considerable reaction with atmospheric carbon dioxide. This alteration has been enhanced by cracking due to shrinkage, allowing the carbonation to penetrate to deeper levels. At deeper levels, however, microcracks produced by alkali-aggregate reaction have also developed, some of which are infilled with silica gel. Although the fine aggregate fraction (granite) cannot be ruled out as a source of alkali-aggregate reaction, in most cases, the alkali-aggregate reaction veins originate, or are mainly associated with, the coarse aggregate (metatuff) fragments. Minor basalt and rhyolite fragments do not appear to be a source of alkali-aggregate reaction.

5. COMPARISON OF AGGREGATES WITH SAMPLES FROM WOO SHEK KOO QUARRY, SHENZHEN

A cursory inspection of rock samples taken from Woo Shek Koo Quarry, Shenzhen, indicates that the quarry rock has identical characteristics to the coarse aggregate used for the concrete examined in this report. The Woo Shek Koo Quarry is located in the Shenzhen Economic Zone just across the border with the HKSAR. The results of geological mapping in the northern part of the HKSAR (Lai *et al.* 1996) strongly suggests that the rock at Woo Shek Koo Quarry correlates with coarse ash crystal tuff of the Tai Mo Shan Formation. This formation is known to contain zones of mylonitic schists and also hosts pockets of iron sulphide mineralization.

6. CONCLUSIONS

(a) Petrographic examination of thin sections and polished slabs of concrete from a footbridge near the KCR Station at Fanling suggests that metatuff used for the coarse aggregate fraction has potential for alkali reaction. The metatuff is strongly foliated, altered and mineralized, with abundant finely recrystallized quartz, strained quartz phenocrysts, and iron sulphide.

(b) Almost all the examined samples show evidence for cracking and carbonation of the cement paste. Carbonation is more strongly disseminated at shallow levels in the concrete, but has penetrated along cracks to deeper levels.

(c) Alkali-silica gel has been positively identified in three of the core samples (Cores D, E, and G) and most of these are at depths of 80-120 mm from the concrete surface. The likely source of the alkali-silica gel is due to reaction between alkaline components in the cement paste and metatuff aggregate fragments.

(d) Iron sulphide (pyrite) in the metatuff fragments provides potential for further defects in the concrete.

(e) The metatuff fragments in the concrete from a footbridge near Fanling KCR Station have identical petrographic characteristics to rock samples from Woo Shek Koo Quarry, Shenzhen.

7. REFERENCES

ASTM (1996a). Standard Practice for Petrographic Examination of Hardened Concrete. Test Designation: C856-95. American Society for Testing Materials.

ASTM (1996b). Standard Descriptive Nomenclature for Constituents of Natural Mineral Aggregates. Test Designation: C294-86 (Reapproved 1991). American Society for Testing Materials.

DOT (1991). Notes for Guidance on the Specification for Highway Works. Department of Transport, UK, 31 p.

Lai, K.W., Campbell, S.D.G. & Shaw, R. (1996). Geology of the Northeastern New Territories. Geotechnical Engineering Office, Hong Kong, 144 p. (Hong Kong Geological Survey Memoir No. 5).

Midgely, H.G. (1958). The staining of concrete by pyrite. Magazine of Concrete Research, Vol. 10, pp 75-78.

RILEM (1993). Petrographic Working Group Report No. RILEM/TC - 106/93/08. RILEM (The International Union of Testing and Research Laboratories for Materials and Structures), 11 p.

LIST OF TABLES

Table 1 - List of Concrete Thin Sections

Sample No. **CLCBK**	**Job Number** **CLROC**	**Depth#** **(mm)**
980517C/2/B	980013A2A 980013A2B	110-120 100-110
980517C/1/T	980013A1A 980013A1B	10-20 0-10
980517D/1/B	980013A4A 980013A4B	104-114 94-104
980517D/1/T	980013A3A 980013A3B	10-20 0-10
980517E/1/B	980013A6A 980013A6B	105-115 95-105
980517E/1/T	980013A5A 980013A5B	10-20 0-10
980517G/1/B	980013A8A 980013A8B	80-90 70-80
980517G/1/T	980013A7A 980013A7B	10-20 0-10

Legend:

The depth for the appropriate thin sections was measured from the wall surface of the concrete core.

LIST OF PLATES

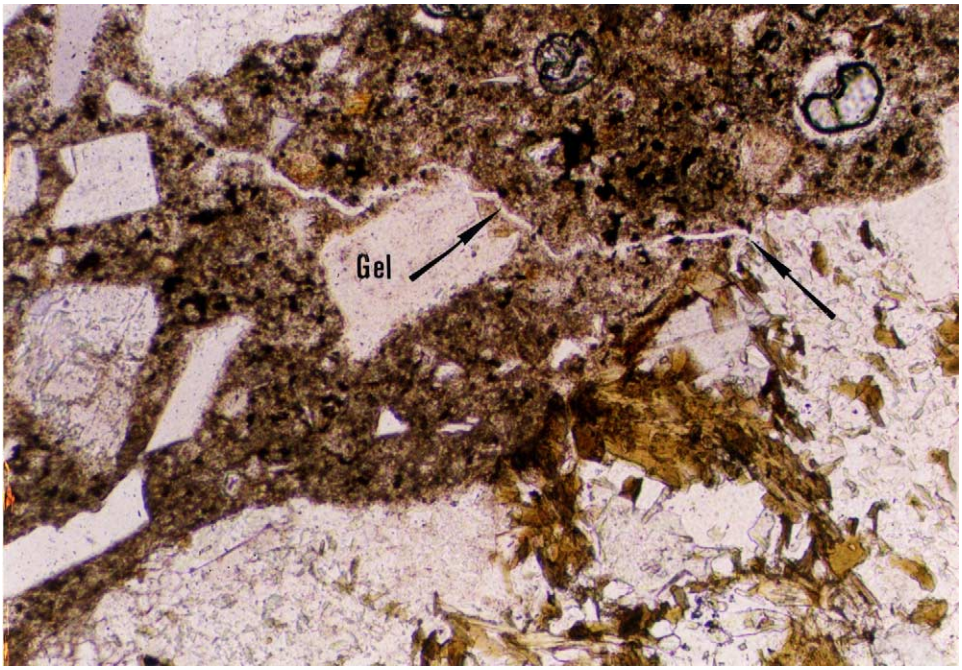

Plate 1 - Microcracks Surrounded by Carbonated Cement in Sample 980013A2A (PPL, Field of View = 1.8 mm) (GS99/035C/05A) (taken on 3.3.99)

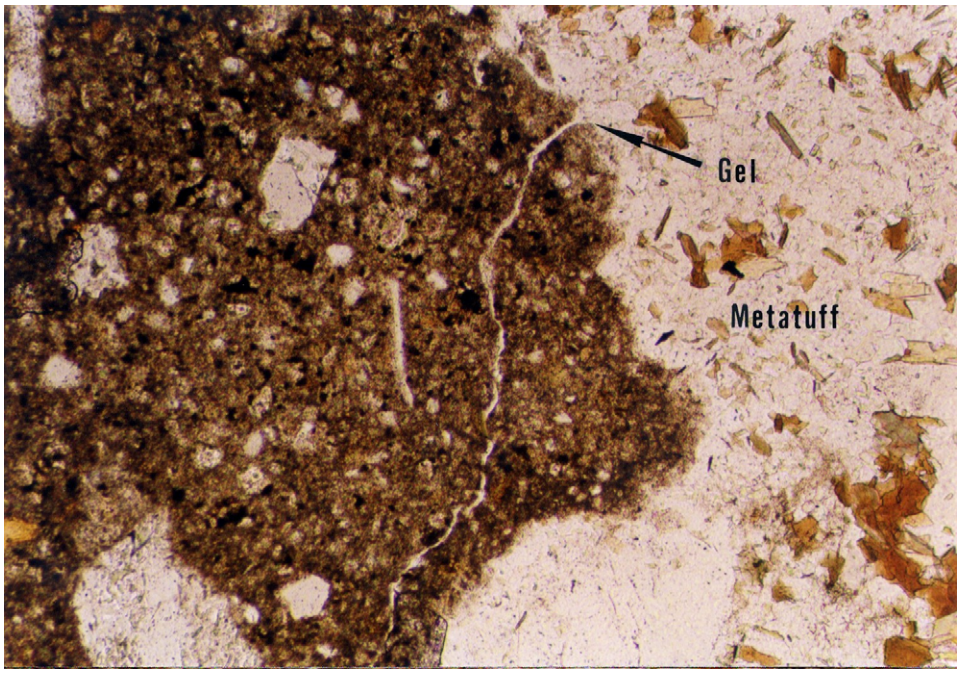

Plate 2 - Microcracks Partly Infilled with Silica Gel and Surrounded by Carbonated Cement Emanating from Metatuff Aggregate Fragment (Sample 980013A4A, PPL, Field of View = 3.6 mm) (GS99/035C/00A) (taken on 3.3.99)

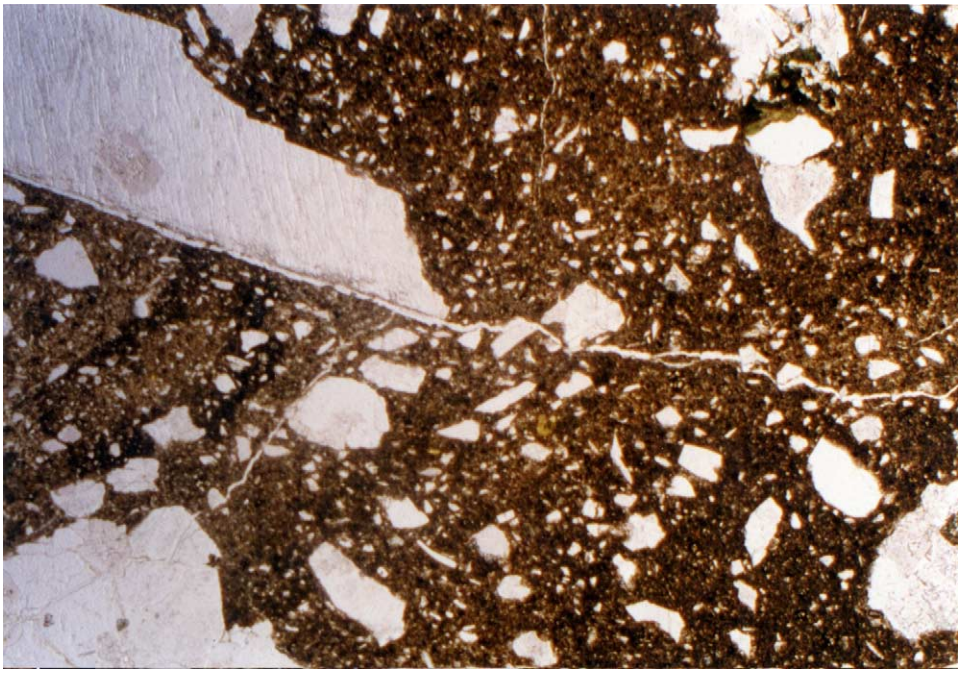

Plate 3 - Microcracks Due to Shrinkage Along Margins of Aggregate Fragments in Sample 980013A5B (PPL, Field of View = 7 mm) (GS99/035C/07A) (taken on 3.3.99)

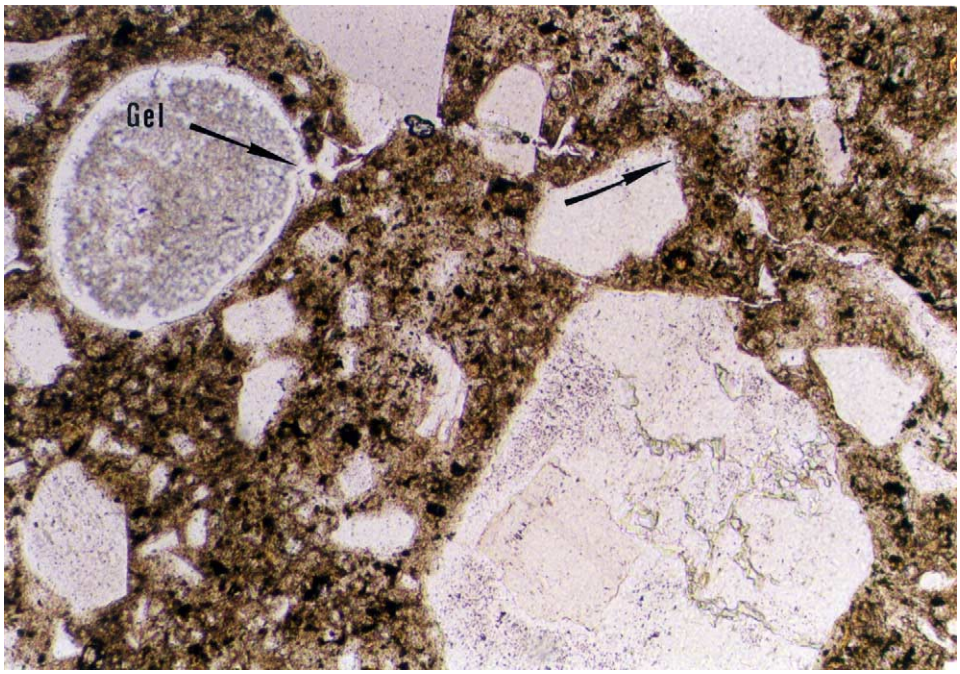

Plate 4 - Microcracks Partly Infilled with Silica Gel Infilling Void in Sample 980013A6A (PPL, Field of View = 1.8 mm) (GS99/035C/09A) (taken on 3.3.99)

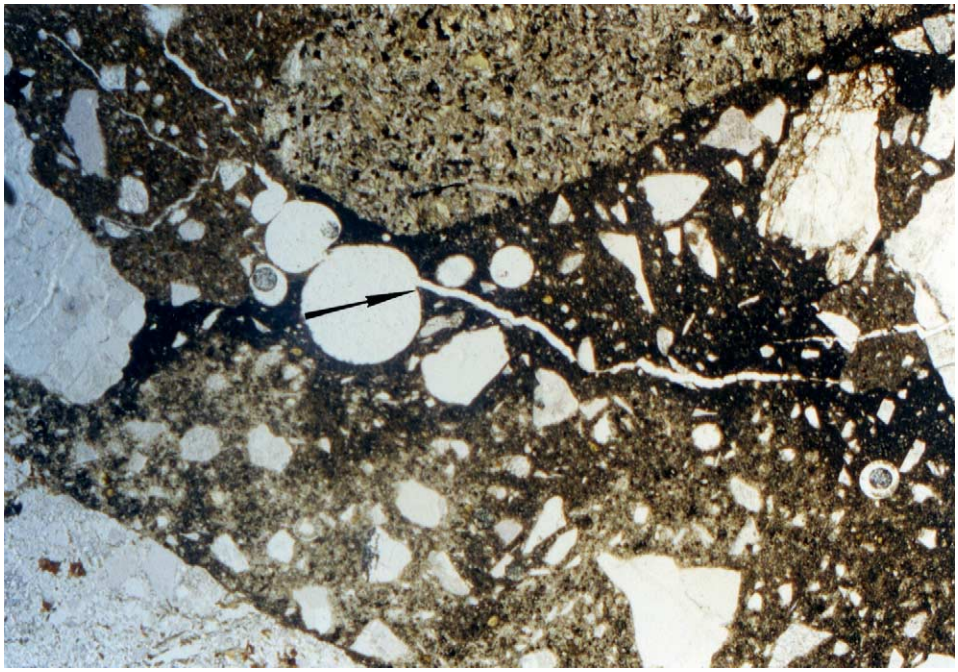

Plate 5a - Microcracks Possibly Due to Shrinkage, Connecting with Voids and Surrounded by Carbonated Cement Paste in Sample 980013A7B. Note Basalt Fragment Below Centre (PPL, Field of View = 7 mm) (GS99/035C/19A) (taken on 3.3.99)

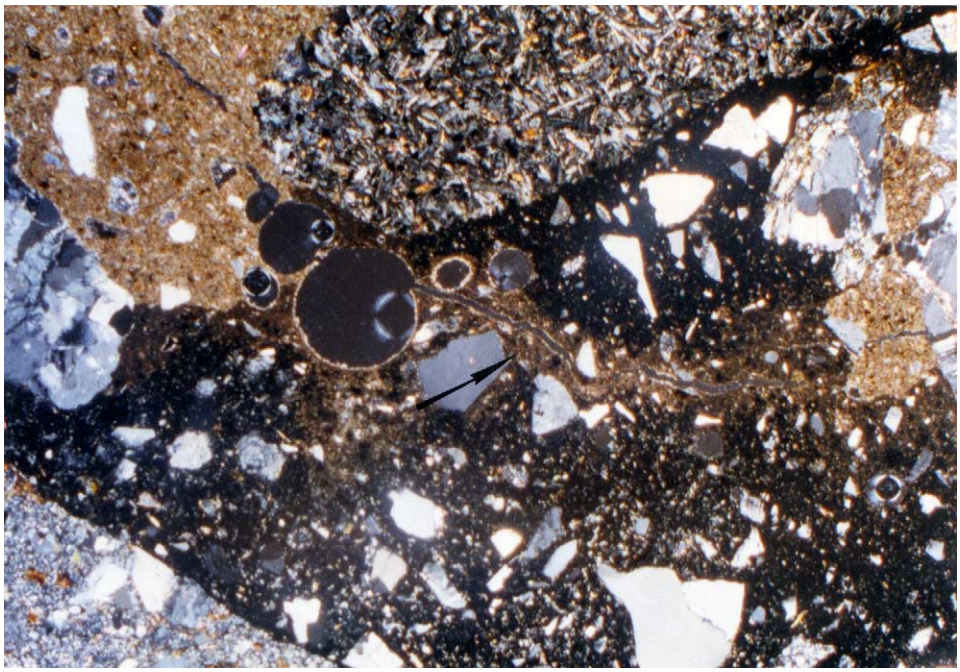

Plate 5b - As for Plate 5a (CPL) (GS99/035C/20A) (taken on 3.3.99)

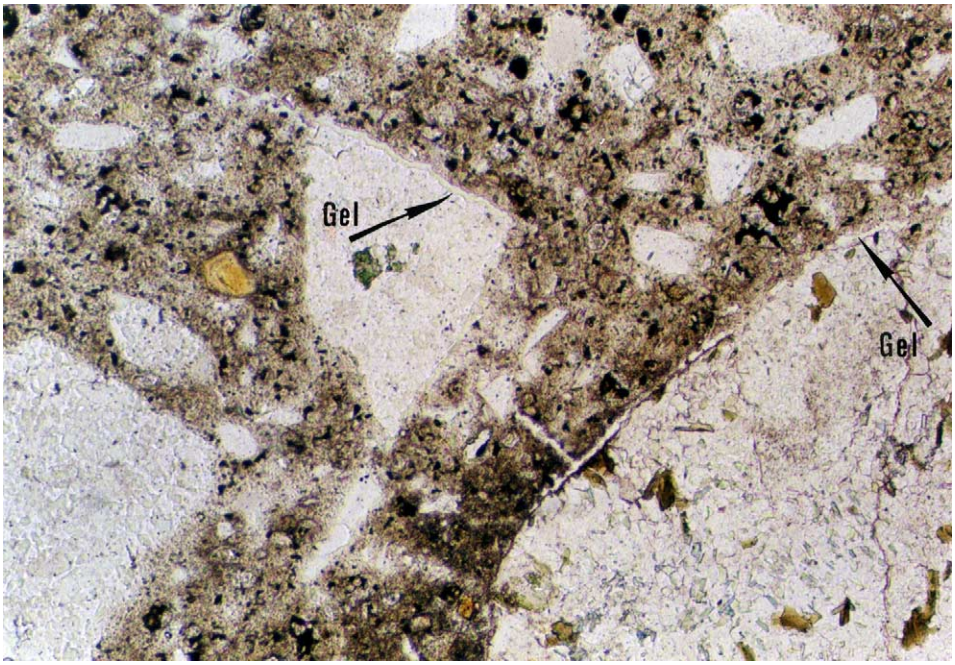

Plate 6 - Silica Gel (Pale Green) in Microveins Surrounding Aggregate Fragments in Sample 980013A8A (PPL, Field of View = 1.8 mm) (GS99/035C/30A) (taken on 3.3.99)

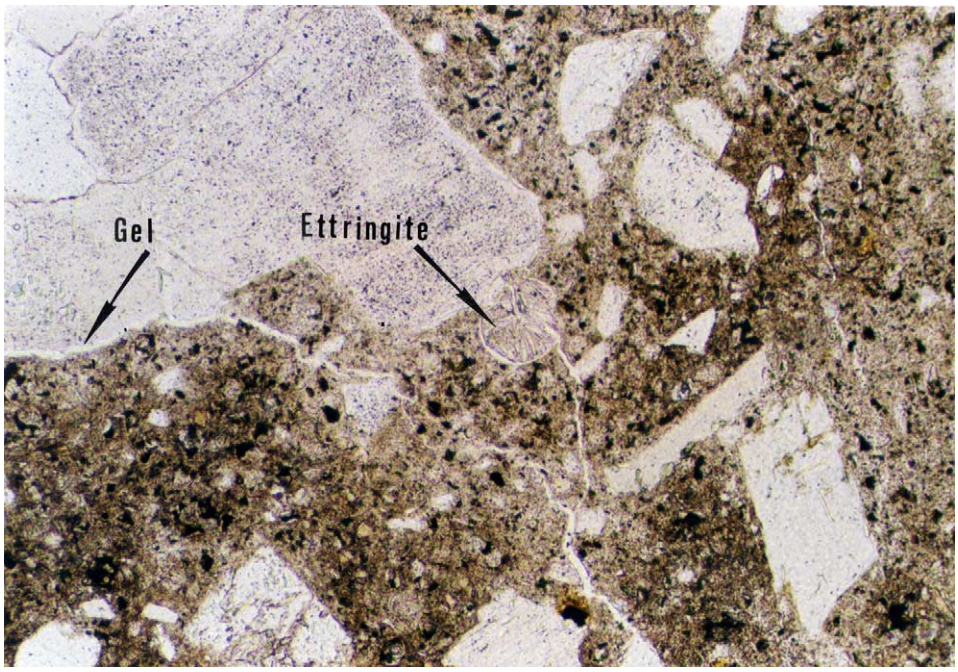

Plate 7 - Veins Infilled with Silica Gel (Pale Green) Cutting Through Cement Paste and Intersecting with Voids Partly Infilled with Ettringite Needles (Sample 980013A8A, PPL, Field of View = 1.8 mm) (GS/99/035C/24A) (taken on 3.3.99)

APPENDIX 1

DETAILED DESCRIPTIONS OF POLISHED SLABS AND THIN SECTIONS

CORE C

A2A	Polished Slab	Coarse aggregate (10-20 mm) is composed of subangular, coarse ash crystal tuff. Fine aggregate (2-5 mm) mostly of granitic clasts. Sand size particles are mostly solitary quartz crystals. Creamy grey matrix. A/B = 20/80.
	Thin Section	Coarse aggregate is mostly altered coarse ash crystal metatuff with a pronounced metamorphic fabric. Carbonate alteration is apparent in tuff clasts, oriented biotite, strained quartz phenocrysts and recrystallized microgranular quartz in matrix. Sericitized feldspars. Granitic fragments not as altered. Microcracks present leading from tuff grains into matrix but no AAR gel positively identified. Cement is fully hydrated, few cement grains, Water/Cement ratio estimated as 0.58.
A2B	Polished Slab	Coarse aggregate (10-20 mm) composed of subangular coarse ash crystal tuff. Fine aggregate (2-5 mm) of granitic clasts. Sand size particles are mostly solitary quartz crystals. Moderately porous as indicated by penetration of resin into matrix. Light grey matrix. A/B = 30/70.
	Thin Section	Coarse aggregate composed of altered coarse ash crystal metatuff. Sericitized feldspar, oriented biotite, strained quartz and recrystallized fine ash matrix. Carbonate alteration in metatuff clasts. Subordinate fine aggregate particles of granite, and rare basalt. Fine cracking of some quartz grains but no obvious AAR.
A1A	Polished Slab	Coarse aggregate (10-20 mm) composed of coarse ash crystal tuff with minor pyrite. Fine aggregate (2-5 mm) of granitic clasts. Numerous voids due to air bubbles in cement. Moderately porous as indicated by infusion of resin into cement. Light grey matrix. A/B = 20/80.
	Thin Section	Coarse aggregate composed of altered coarse ash crystal metatuff. Carbonate replacement, sericitized feldspars, oriented biotite (chloritized) defining a schistocity, recrystallized microcrystalline quartz, strained quartz phenocrysts in aggregate. Very minor veins derived from microcrystalline aggregate particles. Could be infilled by AAR.
A1B	Polished Slab	Coarse aggregate (10-20 mm) composed of subangular coarse ash crystal tuff with minor pyrite. Fine aggregate (5-10 mm) composed of granitic particles. Sand in matrix composed of polycrystalline quartz grains. Fine cracks are present in cement matrix and these are infilled

		with resin. Minor voids due to air bubbles in cement. Minor pyrite. Light grey matrix. A/B = 20/80.
	Thin Section	Coarse aggregate composed of altered coarse ash crystal metatuff. Carbonate replacement, sericitized feldspars, recrystallized microcrystalline quartz in matrix, strained quartz phenocrysts, oriented biotite (commonly chloritized) defining schistocity in some particles. Granite particles are generally fresh but some altered. Cement matrix strongly carbonated in places, some following. No obvious AAR. Microcracks infilled with resin. W/C = 0.58.
CORE D		
A4A	Polished Slab	Coarse aggregate (10-15 mm) composed of subangular to angular coarse ash crystal tuff. Minor pyrite in clasts. Micro-cracking visible in some clasts. Fine aggregate (5-8 mm) composed of tuff clasts. Sand composed mainly of quartz crystals. Brownish grey matrix. Minor voids caused by gas bubbles. A/B = 25/75.
	Thin Section	Coarse aggregate composed of strongly altered coarse ash crystal tuff. Biotite defines schistocity, strained quartz, carbonate alteration. Fine aggregate of altered coarse ash crystal tuff and subrounded rare basalt fragments. Strongly carbonated matrix. Microcracks partly infilled with gel and surrounded by carbonated cement. Carbonation possibly due to thin section making. Source of gel uncertain but often from coarse aggregate particles.
A4B	Polished Slab	Coarse aggregate (10-15 mm) composed of angular coarse ash crystal tuff. Moderately flaky. Minor pyrite. Fine aggregate composed of tuff, and minor basalt particles. Sand composed mainly of quartz. Brownish grey matrix. Minor gas bubbles. A/B = 25/75.
	Thin Section	Coarse aggregate composed of deformed and altered coarse ash crystal tuff. Fine aggregate also composed of mostly of coarse ash crystal tuff particles. Minor basalt. Carbonate alteration in tuff particles, secondary biotite, strained quartz. Microcracks are rare in this specimen. No obvious AAR.
A3A	Polished Slab	Coarse aggregate (8-10 mm) composed of foliated coarse ash crystal tuff. Minor pyrite. Fine aggregate (5-8 mm) composed mainly of tuff clasts. Sand composed of quartz crystals. Voids from air bubbles. Microcracks possibly due to section cutting. Moderately flaky. Yellowish brown matrix. A/B = 25/75.

	Thin Section	Coarse aggregate composed of altered coarse ash crystal tuff. Carbonate replacement, sericitized feldspars, recrystallized quartz in matrix, strained quartz phenocrysts, recrystallized biotite. Fine aggregate composed mostly of tuff clasts but rare basalt clasts. Matrix is strongly carbonated especially surrounded prominent microcracks connecting voids. This suggests that carbonation occurred after cracking.
A3B	Polished Slab	Coarse aggregate (10-15 mm) composed of foliated coarse ash crystal tuff. Minor pyrite. Fine aggregate (5-8 mm) also composed mainly of crystal tuff clasts. Rare basalt clasts. Microcracks connecting voids and infilled with resin. Moderately flaky. Yellowish brown matrix. A/B = 25/75.
	Thin Section	Coarse aggregate composed of altered coarse ash crystal metatuff. Recrystallized quartz in matrix, carbonate replacement, strained quartz phenocrysts, recrystallized biotite. Fine aggregate composed of similar tuff clasts. Rare basalt clasts. Microcracks surrounded by carbonated matrix. Some very altered tuff clasts.
CORE E		
A6A	Polished Slab	Coarse aggregate (10-15 mm) composed of subangular coarse ash crystal tuff. Minor pyrite in tuff particles. Fine aggregate (5-8 mm) composed of granite clasts, with sand fraction composed mostly of polycrystalline quartz. Numerous voids produced by air bubbles. Light grey matrix. A/B = 20/80.
	Thin Section	Coarse aggregate composed of altered coarse ash crystal tuff, carbonate replacement, recrystallized microcrystalline quartz, slightly strained quartz phenocrysts, biotite defines schistocity. Fine aggregate composed of granite clasts. Microcracks possibly infilled with AAR gel.
A6B	Polished Slab	Coarse aggregate (10-20 mm) composed of altered coarse ash crystal tuff. Minor pyrite in tuff clasts. Fine aggregate (5-8 mm) composed of granite fragments, sand fraction composed of quartz crystals. Numerous small gas bubbles. Light grey matrix. A/B = 25/35.
	Thin Section	Coarse aggregate composed of strongly altered coarse ash crystal tuff, carbonate replacement, microcrystalline quartz, slightly strained quartz phenocrysts, secondary growth of biotite (partly chloritized) defining a schistocity in some clasts. Fine aggregate composed of granite fragments. Single grains of subangular quartz. Minor

		cracks infilled with AAR gel. Carbonated areas commonly surround these cracks.
A5A	Polished Slab	Coarse aggregate (10-15 mm) composed of coarse ash crystal tuff. Moderately deformed, minor pyrite. Fine aggregate (5-8 mm) composed of granitic clasts. Moderately flaky. Sand composed of quartz crystals. Minor air bubbles (voids). Whitish grey matrix. A/B = 25/75.
	Thin Section	Coarse aggregate composed of altered coarse ash crystal metatuff, some strongly foliated clasts. Carbonate replacement, recrystallized quartz in matrix, recrystallized biotite, strained quartz phenocrysts. Fine aggregate composed mainly of subangular granitic clasts. Strongly carbonated matrix. Microcracks on margins of aggregates and cutting through. Possibly infilled with gel. Origin uncertain. Carbonation concentrated around microcracks.
A5B	Polished Slab	Coarse aggregate (10-15 mm) composed of partly foliated coarse ash crystal tuff. Minor pyrite. Weakly flaky. Fine aggregate (5-8 mm) composed mainly of granitic clasts. Sand composed of quartz crystals. Microcracks common and filled with resin. Minor air bubbles (voids). Microcracks commonly surround aggregate particles. Brownish white matrix. A/B = 20/80.
	Thin Section	Coarse aggregate composed of altered coarse ash crystal metatuff. Strained quartz phenocrysts, carbonate replacement, recrystallized quartz in matrix and recrystallized biotite. Fine aggregate composed of granitic fragments. Matrix is almost completely carbonated. Thin microcracks surrounded by more finely carbonated matrix. Microcracks cut through whole section, not concentrated on aggregate grain boundaries.
CORE G		
A8A	Polished Slab	Coarse aggregate (10-20 mm) composed of subangular, deformed coarse ash crystal tuff. Pyrite present in deformed aggregate. Fine aggregate (5-8 mm) is mostly granitic clasts. Minor voids due to air bubbles. Sand in matrix is mostly polycrystalline quartz. Light grey matrix. A/B = 20/80.
	Thin Section	Coarse aggregate composed of altered coarse ash crystal tuff which is moderately deformed. Recrystallized biotite, microcrystalline quartz, strained quartz phenocrysts, minor carbonate replacement, sericitized

		feldspars. Granite particles are generally fresh, some containing minor muscovite. Some fresh rhyolite lava fragments. Carbonation of cement along microcracks which intersect air bubbles. Minor ettringite. Minor AAR veins derived from deformed tuff clasts.
A8B	Polished Slab	Coarse aggregate (10-20 mm) composed of subangular, moderately deformed coarse ash crystal tuff. Minor pyrite in strongly deformed tuff particles. Fine aggregate (5-10 mm) composed mostly of granitic particles. Sand size particles in cement composed of polycrystalline quartz. Minor voids due to air bubbles. Microcracks in aggregate particles. Light grey matrix. A/B = 15/85.
	Thin Section	Coarse aggregate composed of moderately to strongly altered coarse ash crystal tuff. Oriented biotite, recrystallized microcrystalline quartz, carbonate replacement, partly strained quartz phenocrysts. Fine aggregate includes granite and rhyolite clasts. Strongly carbonated matrix in places. Lots of ettringite infilling voids, AAR along aggregate boundaries and infilling veins. Microcracks, some infilled with gel, are commonly surrounded by carbonation.
A7A	Polished Slab	Coarse aggregate (10-20 mm) composed of foliated, angular to subangular coarse ash crystal tuff. Moderately flaky. Fine aggregate (5-8 mm) composed of quartz crystals and granite clasts. Sand particles composed of quartz crystals. Sporadic microcracks. Light greyish white matrix. Minor pyrite. A/B = 20/80.
	Thin Section	Coarse aggregate composed of moderately deformed coarse ash crystal tuff. Carbonate replacement, microcrystalline quartz in matrix, strained quartz phenocrysts, recrystallized biotite, sericitized feldspar. Fine aggregate composed of granitic clasts, rare rhyolite lava and basalt. Partly carbonated matrix. Colourless gel infilling microcracks and intersecting voids.
A7B	Polished Slab	Coarse aggregate (10-20 mm) composed of deformed, angular to subangular coarse ash crystal tuff. Some fine ash tuff clasts. Minor pyrite. Slightly foliated clasts. Fine aggregate (5-8 mm) composed of mainly granitic clasts. Sand composed of quartz crystals. Microcracks prominent around coarse aggregate. Infilled with resin. Obvious carbonation associated with cracks. Yellowish white matrix. A/B = 30/70.

Thin Section	Coarse aggregate composed of altered coarse ash crystal metatuff. Carbonate replacement, microcrystalline quarts, recrystallized biotite, strained quartz phenocrysts. Fine aggregate comprises granitic clasts and minor rhyolite clasts. Some recrystallized strained granitic clasts derived from tuff. Minor basalt clasts. Strongly carbonated matrix. Microcracking abundant along aggregate grain boundaries, interlinking with voids and surrounded by carbonation. Some cracks possibly infilled with pale greenish gel but difficult to confirm. Some cracks may originate on granite clasts, but the widest cracks are on the margins of tuff clasts.